Pramana – J. Phys. (2020) 94:115
https://doi.org/10.1007/s12043-020-01962-5

Nonlinear stability analysis of coupled azimuthal interfaces between three rotating magnetic fluids

GALAL M MOATIMID[1] and MARWA H ZEKRY[2,*]

[1]Department of Mathematics, Faculty of Education, Ain Shams University, Roxy, Cairo, Egypt
[2]Department of Mathematics and Computer Science, Faculty of Science, Beni-Suef University, Beni-Suef, Egypt
*Corresponding author. E-mail: marwa.zekry@science.bsu.edu.eg

MS received 14 December 2019; revised 7 March 2020; accepted 9 April 2020

Abstract. The current work deals with the nonlinear azimuthal stability analysis of coupled interfaces between three magnetic fluids. The considered system consists of three incompressible rotating magnetic fluids throughout the porous media. Additionally, the system is pervaded by a uniform azimuthal magnetic field. Therefore, for simplicity, the problem is considered in a planar configuration. The adopted nonlinear approach depends mainly on solving the linear governing equations of motion with the implication of the corresponding convenient nonlinear boundary conditions. The linear stability analysis resulted in a quadratic algebraic equation in the frequency of the surface waves. Consequently, the stability criteria are theoretically analysed. A set of diagrams is plotted to discuss the implication of various physical parameters on the stability profile. On the other hand, the nonlinear stability approach revealed two nonlinear partial differential equations of the Schrödinger type. With the aid of these equations, the stability of the interface deflections is achieved. Subsequently, the stability criteria are theoretically accomplished and numerically confirmed. Regions of stability/instability are addressed to illustrate the implication of various parameters on the stability profile.

Keywords. Nonlinear instability; rotating flow; porous media; magnetic fluids; coupled nonlinear Schrödinger equations.

PACS Nos 47.20.Ib; 68.03.Kn; 47.32.Ef

1. Introduction

Naturally, a material is magnetised by a magnetic field. Simultaneously, the magnitude and direction of this field depend mainly on the structure of the material. In the same vein, Coey's book [1] introduced a review of the classification of magnetism of iron. Ferromagnetic, diamagnetic, paramagnetic, and antimagnetic iron were reviewed in his book. Magnetic materials that are weakly magnetised and do not have any magnetisation are called paramagnetic. In accordance with their valuable applications, the researchers have paid great attention to the topic of magnetic fluids (see Rosensweig [2], whose work discussed the fluid dynamics and science of magnetic liquids). Fluid media, composed of solid magnetic particles of sub-domain size, dispersed in a liquid carrier, are the basis for highly stable, strongly magnetisable liquids known as magnetic fluids or ferrofluids. The fluid dynamics of magnetic fluids differ from that of ordinary fluids in that stress of magnetic origin, appearance and, unlike in magnetohydrodynamics, there need not be electrical currents. Zelazo and Melcher [3] gave a general formulation of incompressible ferrohydrodynamics of a ferrofluid with nonlinear magnetisation. They differentiated clearly between the effects of inhomogeneities in the fluid properties and saturation effects from the non-uniform field. Furthermore, they introduced three experiments to support the theoretical models and emphasise the interface dynamics as well as the stabilising effects of a tangential magnetic field. Using the method of multiple scales, Malik and Singh [4] investigated the nonlinear wave propagation of capillary-gravity waves on the surface of a ferrofluid. The stability analysis reveals the existence of different regions of instability. Moreover, they showed that nonlinear instability cannot be suppressed by the application of a strong magnetic field. Elhefnawy *et al* [5] have done the nonlinear analysis of Rayleigh–Taylor instability of two immiscible, magnetic fluids. They found out that the evolution of the amplitude is governed by

Published online: 30 July 2020

the nonlinear Ginzburg–Landau equation which governs the instability criteria. Consequently, the stability analysis and numerical simulations were achieved to describe linear and nonlinear stages of the interface evolution and to display the stability diagrams. Recently, El-Dib *et al* [6] presented a novel approach to analyse the nonlinear rotating Rayleigh–Taylor instability of two superposed magnetic fluids. Their analysis depends mainly on the homotopy perturbation method. The results showed that the homotopy perturbation method can effectively predict the result of such problems. Eventually, one may use this technique to acquire other expressions of velocities and to interpret the physical situations. Moreover, they performed a numerical calculation to confirm the effects of various parameters in the stability profile.

The stability analysis of a flat interface between two superposed fluids, which are saturated in porous media was first investigated by Bau [7]. He derived the marginal stability criteria for the Darcian as well as non-Darcian fluids. Furthermore, in both cases, the instability occurs if the velocities exceed some critical value. Zakaria *et al* [8] investigated the stability profile of streaming magnetic fluids throughout the porous media. Their model consisted of three incompressible magnetic fluid layers. They showed that the thickness of the middle layer plays a destabilising role in the stability profile. Additionally, dual roles were found to be due to the initial streaming and porosity. Al-Karashi and Gamiel [9] studied the interface stability of three fluid layers. Their media were fully saturated in porous media. Their linear stability approach lead to two-coupled Mathieu equations. They found out the dual role of porosity. Moatimid *et al* [10] investigated the influence of an axial periodic field on streaming flows throughout the three coaxial infinite cylinders. The three fluids are saturated in fully saturated porous media. However, they did not consider the symmetric and antisymmetric modes in their analysis. Furthermore, the numerical calculations indicated that the coefficients of mass and heat transfers as well as streaming have destabilising roles. In contrast, the porosity has a stabilising influence. Recently, Moatimid *et al* [11] introduced a few representatives of porous media in a streaming cylindrical sheet. Their analysis resulted in damped differential equations with complex coefficients. These equations were combined to obtain a single dispersion equation. They showed that Darcy's coefficients, as well as the dielectric constants, played a stabilising influence in the stability picture. Moatimid *et al* [12] investigated the impact of a periodic tangential magnetic field on the stability of a horizontal flat sheet in porous media. The three viscous fluid layers were initially streaming with uniform velocities, and the magnetic field admitted the presence of free surface currents. The governed transition curves (the curves that divide the stability and instability regions) were theoretically obtained and numerically confirmed.

In the case of rotating coaxial infinite cylinders, the Navier–Stokes equations have a stationary solution at which the velocity and pressure depend only on the distance to the axis of rotation (see Kochin *et al* [13]). This solution described the so-called basic flow (Couette flow). Taylor [14] showed that all experiments seem to indicate that in all steady cases, motion is possible if the motion is sufficiently slow. Additionally, many attempts have been made to discover some mathematical representation of fluid instability, but so far they have been unsuccessful in every case. Later, it was shown that this condition is also valid in a more general case, see for instance Synge [15]. Recently, Abakumov [16] presented the mathematical simulation of viscous gas flows between two co-axial rotating concentric cylinders and spheres. The results showed that cylindrical and spherical Couette flows can be studied within the framework of the mathematical viscous gas model by applying direct numerical simulation using explicit finite-difference schemes. The stability of spiral flow when there is a pressure difference in the channel between two coaxial cylinders and rotation of one of the cylinders was investigated by Rudyak and Bord [17]. It is shown that, depending on the azimuthal Reynolds number, the modes with different azimuthal wavenumbers can be more unstable. The data of the calculations are in good agreement with the available experimental data. Recently, El-Dib and Mady [18] investigated the Rayleigh–Taylor instability of two rotating superposed magnetic fields in the presence of vertical and horizontal magnetic flux. The nonlinear stability analysis resulted in a very complicated transcendental characteristic equation. It was constructed as the well-known Duffing equation, simultaneously, with an integration of the dependent variable. In analogy with the integral equations, the authors termed this characteristic equation as an integro-Duffing kind. The homotopy perturbation technique was applied to the nonlinear governing equation of the surface deflection to acquire the stability criteria. Their numerical calculations showed the influence of several physical parameters on the stability profile.

The nonlinear Schrödinger equation is of great importance in many fields of engineering and applied science such as, quantum mechanics, optics, fluid dynamics, plasma physics, molecular biology, magneto-static spin waves etc. Recently, Lu *et al* [19] investigated the generalised nonlinear Schrödinger equation of the third order. They showed that their obtained results may be used in

more nonlinear complex physical phenomena. Liu and Zhang [20] investigated the two main aspects of nonlinear Schrödinger equation. Moreover, all solutions were presented via three-dimensional plots by choosing some special parameters to show the dynamic characteristics. Because of the cubic nonlinear-type of the Schrödinger equation, it has crucial applications. Asadzadeh and Standard [21] analysed the nonlinear Schrödinger equation, based on two-level time stepping scheme with finite spatial discretisation. On the other hand, many researchers addressed nonlinear analysis using the method of multiple time scales. Nayfeh [22] used this approach to acquire two partial differential equations that characterize the evolution of two-dimensional wave-packets of the interface between two superposed ideal fluids. These equations are coupled with each other to give two interchange nonlinear Schrödinger equations. Using these equations, the stability criteria were judged. Elhefnawy [23] has done the nonlinear stability analysis of the Rayleigh–Taylor instability of two superposed magnetic fluids. He showed that the evolution amplitude of the surface wave is judged by a nonlinear Ginzburg–Landau equation. Therefore, the stability criteria were discussed using both analytical and numerical approaches. The nonlinear stability of a cylindrical interface between two fluids was investigated by Lee [24]. Throughout his nonlinear analysis, a nonlinear Ginzburg–Landau equation was obtained. Therefore, the regions of stability and instability were addressed. Zakaria [25] studied the nonlinear stability of the interface between two superposed magnetic fluids in the presence of an oblique magnetic field. His analysis resulted in Schrödinger and Klein–Gordon equations. The existing conditions of the Stokes waves with their instability conditions were combined to achieve the general criteria. He obtained the properties of instability. These conditions were discussed analytically and graphically. El-Dib [26] extended the Nayfeh's approach [22] to derive the nonlinear stability criteria of coupled interfaces. The analysis revealed the case of uniform as well as periodic external fields. His technique resulted in two Schrödinger equations whose combination give the stability criteria. Weakly nonlinear instability of the surface waves propagating between two viscoelastic cylindrical flows was investigated by Moatimid [27]. Typically, a nonlinear Schrödinger equation with complex coefficients was obtained. Therefore, the regions of stability and instability were identified for the wave train disturbances. Elhefnawy *et al* [28] studied the nonlinear instability of finite cylindrical conducting fluids under a radial electric field. They found that the evolution of the amplitude of the surface wave was governed by two partial differential equations. Following Nayfeh's approach [22], they derived two alternate nonlinear Schrödinger equations. Therefore, the stability criteria were analytically discussed and numerically confirmed. Eghbali and Farokhi [29] derived cylindrically and spherically modified nonlinear Schrödinger equation. They showed that the modulation instability of the dust-acoustic waves, in cylindrical and spherical geometries, differs from those in a planar one-dimensional geometry. The nonlinear Rayleigh–Taylor instability of a cylindrical interface between two-phase fluids was examined by Seadawy and El-Rashidy [30]. They showed that the phases enclosed between the coaxial cylindrical surface are transformed in the form of the Schrödinger equation with complex coefficients. By means of the F expansion method, they achieved an exact solution of the nonlinear Landau–Ginzburg equation. Zhang *et al* [31] derived exact solutions of new special forms of coupled famous Klein–Gordon–Zakharov equations. Furthermore, they derived a subsidiary higher-order ordinary differential equation with the positive fractional power terms. Recently, Moatimid *et al* [32] investigated the nonlinear instability of a cylindrical interface between two magnetic fluids in porous media. The coupling of the Laplace transforms and homotopy perturbation techniques were adopted to obtain an approximate analytical solution of the interface profile. The nonlinear stability analysis resulted in two levels of solvability conditions. Using these conditions, a Ginzburg–Landau equation was derived.

As per the authors' knowledge, this is the first time that the nonlinear stability analysis of coupled interfaces is studied. Therefore, the current work deals with the investigation of the nonlinear stability analysis of coupled interfaces. An azimuthal uniform magnetic field is applied on the tangent of the circular cross-sections. The case of a periodic field will be considered in a subsequent paper. Therefore, the current manuscript gives an extension to our previous work [33]. The aim of the work is to discuss the nonlinear stability of two rotating columns. For simplicity, the analysis is performed in two non-axisymmetric perturbations. The rest of the paper is organised as follows: Section 2 is devoted to the methodology of the problem. In this section, the equations of motion and the appropriate nonlinear boundary conditions are presented. The linear stability analysis is given in §3. In this section, the theoretical stability criteria are depicted. The nonlinear stability approach is presented in §4. In this section, the derivation of the coupled nonlinear Schrödinger equations and the nonlinear stability criteria are illustrated. Additionally, the numerical discussions of the previous stability criteria are introduced. Finally, the concluding remarks are summarised in §5.

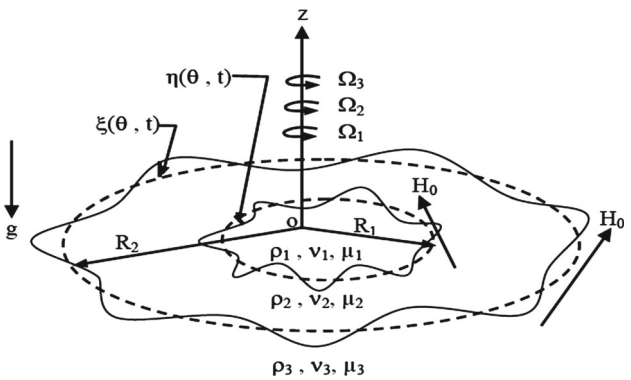

Figure 1. Sketch of the physical model.

2. Methodology of the problem

Vertical cylindrical flows consisting of three incompressible homogeneous magnetised fluid columns of infinite length are considered. Throughout this formulation, the subscripts 1, 2 and 3 denote the parameters associated with the inner, middle and outer fluids, respectively. For more convenience, the work considered the cylindrical polar coordinates. In the equilibrium configuration, the interface surfaces are assumed to be of circular cross-sections with the radii R_1 and R_2. The fluids are saturated throughout the porous media. For simplicity, the porosities of the media are considered as unity. The inner column performs a rigid-fluid rotation, in a weightless condition, with a uniform angular velocity Ω_1 about its axis of symmetry. This column has density ρ_1, Darcy coefficient ν_1, and magnetic permeability μ_1. The middle column has density ρ_2, Darcy coefficient ν_2, magnetic permeability μ_2 and constant angular velocity Ω_2. The outer one is considered as an unbounded fluid having density ρ_3, Darcy coefficient ν_3, magnetic permeability μ_3 and constant angular velocity Ω_3. The three fluids are assumed to be affected by an azimuthal uniform magnetic field H_0. No surface currents are assumed to be present at the surface of separation. The gravitational acceleration g, along the negative z direction is taken into consideration. The fluids exhibit interface surface tensions, where T_1 and T_2 are the amount of the surface tensions in the inner and outer surface, respectively. A schematic diagram of the configuration of the physical model is given in figure 1.

As stated in the Abstract, the following weakly nonlinear analysis depends mainly on solving the linear governing equation of motion, together with the implication of the nonlinear boundary conditions. For simplicity and without any loss of generality, the problem is considered in two dimensions. In other words, the physical model lies in a horizontal plane at some value of the z coordinate. Typically, as given in the pioneer book of Chandrasekhar [34], if a small but finite departure from the equilibrium position at the two interfaces is considered, one finds the following interface perturbations:

The inner and outer surfaces are given by

$$r = R_1 + \eta(\theta, t), \tag{1a}$$

$$r = R_2 + \xi(\theta, t), \tag{1b}$$

where $\eta(\theta, t)$ and $\xi(\theta, t)$ are general unknown functions representing the surface deflection behaviour. Therefore, after a small departure from the equilibrium state, the interface profiles may be expressed as

$$S_1(r, \theta; t) = r - R_1 - \eta(\theta, t) \tag{2a}$$

and

$$S_2(r, \theta; t) = r - R_2 - \xi(\theta, t). \tag{2b}$$

Therefore, the unit outward normal vector of the interfaces may be written as

$$\underline{n}_1 = \nabla S_1 / |\nabla S_1| = \left(\underline{e}_r - \frac{1}{r}\eta_\theta \underline{e}_\theta\right)\left(1 + \frac{1}{r^2}\eta_\theta^2\right)^{-1/2} \tag{3a}$$

and

$$\underline{n}_2 = \nabla S_2 / |\nabla S_2| = \left(\underline{e}_r - \frac{1}{r}\xi_\theta \underline{e}_\theta\right)\left(1 + \frac{1}{r^2}\xi_\theta^2\right)^{-1/2} \tag{3b}$$

where $\underline{e}_r$ and $\underline{e}_\theta$ are unit vectors along the r and θ directions, respectively.

The angular velocity of the fluids is given as $\underline{\Omega} = \Omega \underline{e}_z$. It is convenient to write the governing equation of motion in this frame of reference, which rotates with an angular velocity $\underline{\Omega}$ as follows:

$$\left(\frac{\partial \underline{V}_j}{\partial t} + (\underline{V}_j \cdot \nabla)\underline{V}_j + 2(\underline{\Omega}_j \times \underline{V}_j) - \frac{1}{2}\nabla\left|(\underline{\Omega}_j \times \underline{r})^2\right|\right) = -\frac{1}{\rho_j}\nabla P_j - \nu_j \underline{V}_j - g\underline{e}_z,\ j = 1, 2, 3, \tag{4}$$

where $V_j = V_j(r, \theta; t)$ is the fluid velocity, P_j represents the pressure, and $\underline{e}_z$ is the unit vector along the z direction. The third and fourth terms, on the left-hand side of the equation of motion, are the Coriolis force and the centrifugal implication, respectively.

Now, consider the function π_j which represents the increment of the pressure, sometimes called the reduced pressure. It may be written as follows:

$$\pi_j = p_j - \frac{1}{2}\rho_j(\underline{\Omega}_j \wedge \underline{r})^2. \tag{5}$$

Therefore,

$$\left(\frac{\partial \underline{V}_j}{\partial t} + (\underline{V}_j \cdot \nabla)\underline{V}_j + 2(\underline{\Omega}_j \times \underline{V}_j)\right) = -\frac{1}{\rho_j}\nabla\pi_j - \nu_j \underline{V}_j - g\underline{e}_z, \quad j = 1, 2, 3. \tag{6}$$

The incompressibility condition yields

$$\nabla \cdot \underline{V} = 0. \tag{7}$$

In the present work, the Kelvin–Helmholtz model is adopted, so that the total velocity vector may be represented as $\underline{V}(u, v_0 + v, w)$, where $v_0 = r\Omega$ is the unperturbed velocity. Only two-dimensional disturbances are considered without any generality loss. Therefore, one may assume that $w = 0$. The zero-order solution of eq. (6) yields

$$\pi_{0j} = -\rho_j g z + \lambda_j, \tag{8}$$

where λ_j is the time-dependent integration function.

In light of the normal mode analysis, see for instance Chandrasekhar [34], in the two-dimensional flow, any perturbed function may be represented in the following form:

$$F(r,\ \theta;\ t) = \hat{f}(r;\ t)\mathrm{e}^{im\theta}, \tag{9}$$

where F stands for any linear physical quantity.

For the two-dimensional flow, the linearised planer equations of motion may be written as follows:

$$Du - 4\Omega v = -\frac{1}{\rho}\frac{\partial \pi}{\partial r} \tag{10}$$

and

$$Dv + 4\Omega u = -\frac{im}{\rho r}\pi \tag{11}$$

together with the following incompressibility condition

$$\frac{\partial u}{\partial r} + \frac{im}{r}v + \frac{u}{r} = 0, \tag{12}$$

where the operator D is defined as

$$D \equiv \frac{\partial}{\partial t} + im\Omega + \nu.$$

Typically, the validation of eq. (12) needs a stream function $\phi\ (r, \theta; t)$, such that

$$u = -\frac{im}{r}\phi \quad \text{and} \quad v = \frac{\partial \phi}{\partial r}. \tag{13}$$

The stream function may be determined by eliminating the pressure from the equations of motion. For this purpose, the combination of eqs (10), (11) and (12), yields

$$\left(r^2\frac{\partial^2}{\partial r^2} + r\frac{\partial}{\partial r} - m^2\right) D\hat{\phi}(r, t) = 0, \tag{14}$$

which has the following solution:

$$D\hat{\phi}(r, t) = A_1^*(t)r^m + A_2^*(t)r^{-m}. \tag{15}$$

In order to obtain the finite solutions, one gets

$$\phi_1(r, \theta, t) = A_1\,(t)\, r^m \mathrm{e}^{im\theta}, \quad r \le R_1, \tag{16a}$$

$$\phi_2(r,\theta,t) = \left(A_2\,(t)\, r^m + A_3\,(t)\, r^{-m}\right)\mathrm{e}^{im\theta}, \quad R_1 \le r \le R_2 \tag{16b}$$

and

$$\phi_3(r, \theta, t) = A_4\,(t)\, r^{-m}\mathrm{e}^{im\theta}, \quad r \ge R_2, \tag{16c}$$

where

$$A_j(t) = D^{-1}A_j^*\,(t)\,, \quad j = 1, 2, 3, 4. \tag{17}$$

Here $A_j(t)$ is an arbitrary time-dependent function. They may be defined from the appropriate nonlinear boundary conditions.

The integration of the linear governing equation of motion (6) resulted in the distribution function of the pressure as given by

$$\pi_j = \frac{\rho_j}{m}\left(ir\frac{\partial^2\phi_j}{\partial r\partial t} + r(i\nu_j - m\Omega_j)\frac{\partial\phi_j}{\partial r} + 2m\Omega_j\phi_j\right). \tag{18}$$

According to the Maxwell equations; for an instance, see Melcher [35], the quasi-static approximation will be applied to ignore the influence of the electric field. Therefore, the governing equations of motion of the magnetic field may be formulated as follows:

$$\nabla \cdot \mu_j \underline{H}_j = 0 \tag{19}$$

and

$$\nabla \times \underline{H}_j = \underline{0}. \tag{20}$$

As given in the formulation of the problem, no surface currents are assumed to be present at the surface of separation. Therefore, the magnetic field may be expressed in terms of the scalar magnetostatic potentials $\psi_j(r, \theta; t)$, i.e., $\underline{H}_j = H_0\underline{e}_\theta - \nabla\psi_j(r, \theta; t)$, such that the total perturbed magnetic fields can be expressed as

$$\underline{H}_j = -\frac{\partial\psi_j}{\partial r}\underline{e}_r - \frac{1}{r}\left(\frac{\partial\psi_j}{\partial\theta} - H_0\right)\underline{e}_\theta. \tag{21}$$

The combination of eqs (19) and (20) yields

$$\nabla^2\psi_j = 0. \tag{22}$$

In accordance with the two-dimensional flow considered here, the Laplace's equation as given in eq. (22) and governs the magnetic potential ψ_j may be written as

$$\left(r^2\frac{\partial^2}{\partial r^2} + r\frac{\partial}{\partial r} - m^2\right)\hat{\psi}(r, t) = 0, \tag{23}$$

which has the following solutions:

$$\psi_1(r,\theta,t) = B_1(t)\, r^m e^{im\theta}, \quad r \le R_1, \tag{24a}$$

$$\psi_2(r,\theta,t) = \left(B_2(t)\, r^m + B_3(t)\, r^{-m}\right) e^{im\theta}, \quad R_1 \le r \le R_2 \tag{24b}$$

and

$$\psi_3(r,\theta,t) = B_4(t)\, r^{-m} e^{im\theta}, \quad r \ge R_2, \tag{24c}$$

where $B_j(t)$ is the time-dependent function to be determined from the appropriate nonlinear boundary conditions.

2.1 *Nonlinear boundary conditions*

The general solutions of velocity, pressure and magnetic potential distribution functions, as given in eqs (16a)–(16c), (18) and (24a)–(24c), must satisfy the following appropriate nonlinear boundary conditions:

2.1.1 *At the free interfaces* $r = R_1 + \eta(\theta;t)$ *and* $r = R_2 + \xi(\theta;t)$.

1. The conservation of mass across the interface, which is the so-called kinematic condition, yields

$$\frac{DS_1}{Dt} = 0 \ \text{ at } r = R_1 + \eta(\theta;t) \tag{25}$$

and

$$\frac{DS_2}{Dt} = 0 \ \text{ at } r = R_2 + \xi(\theta;t), \tag{26}$$

where D/Dt represents the material derivative operator.

2. The jump of the tangential components of the magnetic field is continuous at the interface, to yield

$$\underline{n}_j \times \left\| \underline{H}_j \right\| = \underline{0}, \quad j = 1,2,3, \tag{27}$$

where $\|*\| = *_{j+1} - *_j$ denotes the jump due to the external and internal fluid layers, respectively.

3. The jump of the normal components of the magnetic field is continuous at the interface, to give

$$\underline{n}_j . \left\| \mu_j \underline{H}_j \right\| = 0, \quad j = 1,2,3. \tag{28}$$

At this stage, on substituting eqs (16a)–(16c) and (24a)–(24c) into eqs (25)–(28), one finds special solutions, which are consistent with the foregoing nonlinear boundary conditions. They can be written as follows:

$$\phi_1 = -\frac{R_1^2(\eta_t + \Omega_1\eta_\theta)}{m(iR_1 + \eta_\theta)}\left(\frac{r}{R_1}\right)^m, \tag{29}$$

$$\phi_2 = \frac{1}{\Gamma}\big(R_1^{2+m}(R_2 + i\xi_\theta)(\eta_t + \Omega_2\eta_\theta) - R_2^{2+m}(R_1 + i\eta_\theta)(\xi_t + \Omega_2\xi_\theta)\big) r^m$$
$$+ \frac{1}{\Gamma}\big(R_1^{2m}R_2^{2+m}(R_1 - i\eta_\theta)(\xi_t + \Omega_2\xi_\theta) - R_2^{2m}R_1^{2+m}(R_2 - i\xi_\theta)(\eta_t + \Omega_2\eta_\theta)\big) r^{-m}, \tag{30}$$

$$\phi_3 = \frac{R_2^2(\xi_t + \Omega_3\xi_\theta)}{m(-iR_2 + \xi_\theta)}\left(\frac{r}{R_2}\right)^{-m}, \tag{31}$$

$$\psi_1 = -\frac{H_0}{\Lambda(R_1 - i\eta_\theta)}\big(R_1^{1+2m}(\mu_1 - \mu_2)(\mu_2 - \mu_3)(R_2 + i\xi_\theta)(R_1 - i\eta_\theta)\eta_\theta + R_1R_2^{2m}(\mu_1 - \mu_2)(\mu_2 + \mu_3)(R_2 - i\xi_\theta) \times (R_1 + i\eta_\theta)\eta_\theta + 2R_1^mR_2^{1+m}\mu_2(\mu_2 - \mu_3) \times (R_1^2 + \eta_\theta^2)\xi_\theta\big)\left(\frac{r}{R_1}\right)^m, \tag{32}$$

$$\psi_2 = \frac{H_0}{\Lambda}\big(-(\mu_2 - \mu_3)\big((\mu_1 + \mu_2)R_2^{1+m}(R_1 + i\eta_\theta)\xi_\theta + (\mu_1 - \mu_2)R_1^{1+m}(R_1 + i\xi_\theta)\eta_\theta\big) r^m + \big((\mu_1 - \mu_2)R_1^mR_2^m \times \big(R_1^mR_2(\mu_2 - \mu_3)(R_1 - i\eta_\theta)\xi_\theta - (\mu_2 + \mu_3)R_2^mR_1(R_2 - i\xi_\theta)\eta_\theta\big)\big) r^{-m}\big) \tag{33}$$

and

$$\psi_3 = \frac{H_0}{\Lambda(R_2 + i\xi_\theta)}\big(R_2R_1^{2m}(\mu_1 - \mu_2)(\mu_2 - \mu_3)(R_2 + i\xi_\theta)(R_1 - i\eta_\theta)\xi_\theta - R_2^{1+2m}(\mu_1 + \mu_2) \times (\mu_2 + \mu_3)(R_2 - i\xi_\theta)(R_1 + i\eta_\theta)\xi_\theta - 2R_1^{1+m}R_2^m\mu_2(\mu_1 - \mu_2)(R_2^2 + \xi_\theta^2)\eta_\theta\big)\left(\frac{r}{R_2}\right)^{-m}. \tag{34}$$

To study the stability of the system, the remaining boundary condition arises from the normal component of the stress tensor. In accordance with the presence of the amount of surface tensions, this normal component must be discontinuous. The total stress tensor can be formulated as follows:

$$\sigma_{ij} = -\pi\delta_{ij} + \mu H_iH_j - \frac{1}{2}\mu H^2\delta_{ij}, \tag{35}$$

where δ_{ij} is the Kronecker delta

$$\left\| \underline{n}_j \cdot \underline{F}_j \right\| = T_i \nabla \cdot \underline{n}_j, \quad i = 1,2. \tag{36}$$

$\underline{F}_j$ is the total force acting on the interfaces, which is defined as

$$\underline{F} = \begin{pmatrix} \sigma_{rr} & \sigma_{r\theta} \\ \sigma_{\theta r} & \sigma_{\theta\theta} \end{pmatrix} \begin{pmatrix} n_r \\ n_\theta \end{pmatrix}, \tag{37}$$

where n_r, n_θ are the components of the outward unit normal vector $\underline{n}$, along with the r and θ components, respectively.

On substituting from the foregoing outcomes in eq. (36), after lengthy, but straightforward calculation, one gets the following nonlinear characteristic equations:

$$L_1\eta + L_2\xi = N_1(\eta, \xi) \tag{38a}$$

and

$$L_3\eta + L_4\xi = N_2(\eta, \xi), \tag{38b}$$

where the operator L_i is defined as

$$L_i = a_i\frac{\partial^2}{\partial t^2} + b_i\frac{\partial^2}{\partial\theta^2} + c_i\frac{\partial^2}{\partial\theta\partial t} + (h_i + ik_i)\frac{\partial}{\partial t} + (g_i + if_i)\frac{\partial}{\partial\theta}.$$

In addition, the nonlinear terms $N_1(\eta, \xi)$ and $N_2(\eta, \xi)$ represent all the quadratic and cubic terms of the interface deflections η and ξ, a_i, b_i, c_i, h_i, k_i, g_i and f_i are constants involving all the physical characteristics of the problem at hand.

From the zero-order of the normal stress tensor, one gets

$$\lambda_2 - \lambda_1 = (\rho_2 - \rho_1)gz - \frac{T_1}{R_1} + \frac{1}{2}H_0^2(\mu_2 - \mu_1) \tag{39a}$$

and

$$\lambda_3 - \lambda_2 = (\rho_3 - \rho_2)gz - \frac{T_2}{R_2} + \frac{1}{2}H_0^2(\mu_3 - \mu_2). \tag{39b}$$

It is worthwhile to conclude a special case from the previous coupled equations (38a) and (38b) as follows: This case can be obtained here, by setting [36], $\eta_1 = \eta_2 = 0$ and $\omega = 0$. This case can be obtained here by setting $\eta(\theta, t) = \xi(\theta, t)$, $R_1 = R_2$, $T_1 = T_2$, $\nu_1 = \nu_2 = 0$ and then adding eqs (38a) and (38b).

The stability analysis of the current work, throughout using the linear as well as the nonlinear approach, depends mainly on studying the nonlinear characteristic equations as given in (38a) and (38b). The following analysis will be based on the theoretical analysis as given by El-Dib [26].

3. The linear stability approach

Before dealing with the general case, for more convenience, the stability analysis will be examined using a linear point of view. Along with this approach, the linearised analysis of the nonlinear equations given by eqs (38a) and (38b) arises by ignoring the nonlinear terms of the surface elevation.

Therefore, the linearised dispersion equations can be written as follows:

$$L_1\eta + L_2\xi = 0 \tag{40a}$$

and

$$L_3\eta + L_4\xi = 0. \tag{40b}$$

Suppose that a uniform monochromatic wave train solution of eqs (40a) and (40b) is in the following form:

$$\eta(\theta, t) = \gamma_1(t)\mathrm{e}^{im\theta} + \text{c.c.} \tag{41a}$$

and

$$\xi(\theta, t) = \gamma_2(t)\,\mathrm{e}^{im\theta} + \text{c.c.}, \tag{41b}$$

where $\gamma_1(t)$ and $\gamma_2(t)$ are the arbitrary time-dependent functions, which determine the behaviour of the amplitude of disturbance on the interfaces.

Substitute eqs (41a) and (41b) into eqs (40a) and (40b), then separate the real and imaginary parts. The separation of the real and imaginary parts is urgent. After this separation, considering the imaginary parts only, the resulting equations may be solved for ξ_t and η_t, and then substitute them to the real parts. The calculations are not complicated. This procedure resulted in the following linear characteristic second-order differential equation:

$$\gamma_{tt1} + \gamma_1 + \gamma_2 = 0 \tag{42a}$$

and

$$\gamma_{tt2} + \gamma_2 + \gamma_1 = 0. \tag{42b}$$

Equations (42a) and (42b) are linear and homogeneous differential equations with constant coefficients. It follows that the exponential solution is valid. Therefore, one may assume the following solution:

Let

$$\gamma_1(t) = \delta_1\mathrm{e}^{-i\omega t} + \text{c.c.} \tag{43a}$$

and

$$\gamma_2(t) = \delta_2\mathrm{e}^{-i\omega t} + \text{c.c.}, \tag{43b}$$

where δ_j is a real and finite constant.

For the non-trivial solutions of γ_1 and γ_2 that appear in eqs (42a) and (42b), the determinant of the coefficient matrix must be cancelled. This procedure gives the following dispersion relation:

$$\omega^4 + \alpha_1\omega^2 + \alpha_2 = 0, \tag{44}$$

where the coefficients α_1 and α_2 are well-known from the background of the paper. They involved all the physical parameters of the problem in hand. To avoid the length of the paper, they will be omitted.

Actually, the dispersion relation, which is the so-called dispersion relation of the surface waves in the

linear approach, represents a quadratic equation in ω^2. The stability requires that all four roots of ω's must be of real values, i.e. ω^2 should be positive and real. On the basis of eq. (44), it is easily verified that this implies the following criteria:

$$\alpha_1 < 0, \tag{45}$$

$$\alpha_2 > 0 \tag{46}$$

and

$$\alpha_1^2 - 4\alpha_2 > 0. \tag{47}$$

The focus now is on the effect of magnetic field strength on the stability configuration. Consequently, the magnetic field intensity vs. the second radius R_2 will be sketched instead of the wave number of the surface wave. Therefore, it is convenient to rewrite the stability criteria in terms of the magnetic field strength H_0^2. Consequently, the inequalities (45)–(47) may be written as follows:

$$q_1 H_0^2 + q_0 < 0, \tag{48}$$

$$p_2 H_0^4 + p_1 H_0^2 + p_0 > 0 \tag{49}$$

and

$$w_2 H_0^4 + w_1 H_0^2 + w_0 > 0, \tag{50}$$

where the coefficients and w_2 are well-known from the background of the paper. They involved all the physical parameters of the problem. To avoid the length of the paper, they will be omitted.

The inspection of conditions (48)–(50) shows that all of them depend on H_0^2. Before dealing with the numerical calculations and for more convenience, these stability criteria may be rewritten in an appropriate non-dimensional form. This can be done in a number of ways depending on the choice of characteristics of length, time and mass. For this purpose, consider that the parameters g/ω^2, $1/\omega$ and $\rho_2 g^3/\omega^6$ refer to the characteristics of length, time and mass, respectively. The other non-dimensional quantities may be given as

$$\rho_j = \rho_j^* \rho_2, \quad H_0^2 = \frac{H_0^{*2}\rho_2 g^2}{\omega^2 \mu_2}, \quad T_j = \frac{T_j^* \rho_2 g^3}{\omega^4},$$

$$\Omega_j = \frac{\Omega_j^* \Omega_2}{\omega}, \quad \nu_j = \frac{\nu_j^* \nu_2}{\omega}$$

and

$$R_i = R_i^* g/\omega^2.$$

From now on, the asterisk mark may be cancelled, for simplicity, in the following analysis.

It is useful to plot the magnetic field intensity $\log H_0^2$ vs. the outer radius R_2. The effect of the magnetic field strength depends mainly on the signs of the parameters of the leading coefficients of the previous criteria (q_1, p_2 and w_2). Subsequently, the tangential magnetic field has a stabilising influence, if both p_2 and w_2 are positive, and meanwhile, q_1 becomes negative. It follows that the magnetic field has a stabilising influence. The numerical calculations ensure this significance. Therefore, the tangential magnetic field plays a stabilising influence. Typically, this is an early result. It is first confirmed by many researchers; for instance, see refs [10,24].

In what follows, a numerical calculation is done to indicate the influence of various parameters on the stability configuration. In figures 2–7 the transition curves that appear in equalities (48)–(50) are plotted. In these figures, the stable region is denoted by the letter S, whereas the letter U stands for the unstable one. The following calculations considered optional values, whose particulars are

$$\rho_1 = 2,\ \rho_3 = 0.5, \mu_1 = 3, \mu_3 = 0.9,$$

$$\nu_1 = 0.3, \nu_3 = 1.5, \Omega_1 = 0.7,$$

$$\Omega_3 = 0.3, R_1 = 1, T_1 = 0.5, T_2 = 1.3 \text{ and } m = 2.$$

Consequently, R_2 starts from 1.01. In accordance with these numerical values, it is found that inequality (50) is automatically satisfied. Subsequently, it has no implication in the stability picture. Meanwhile, the first two equalities (48) and (49) have three positive roots. Therefore, one gets three transition curves. Equality (48) is plotted as a dotted curve. Equality (49) is plotted to give two solid curves. The calculations showed that q_1 is negative. Therefore, the region above this curve is a stable region and it is denoted by the letter S_1. In contrast, the region below this curve, which is denoted by letter U_1 becomes an unstable region. On the other hand, the calculations showed that the leading coefficient p_2 has a positive sign. Mathematically, the equality of relation (49) is quadratic in H_0^2. Actually, it has two real and distinct roots, say H_1^* and H_2^*. Consider $H_2^* > H_1^*$. When $p_2 > 0$, stability occurs if $H_0^2 > H_2^*$ or $H_0^2 < H_1^*$. On the other hand, when $p_2 < 0$, the stability occurs if $H_1^* < H_0^2 < H_2^*$. Consequently, the stable regions lie above the upper curve, together with the region below the lower curve. These regions are labelled by the letter S_2. Simultaneously, the region bounded between these two curves becomes an unstable region. It is denoted by the letter U_2. These observations are plotted in figure 2.

Figure 2 is plotted to indicate the previous transition curves. As shown from the foregoing discussions, the stability of the system is judged by the upper solid curve. Therefore, the other two curves have no implication in the stability configuration. Consequently, to indicate the

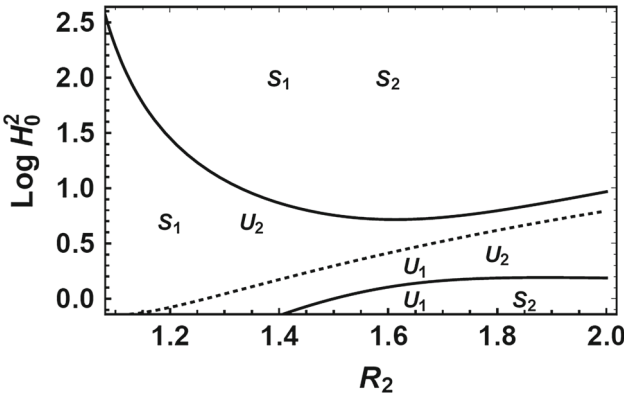

Figure 2. Plots of the linear stability given in inequalities (48) and (49).

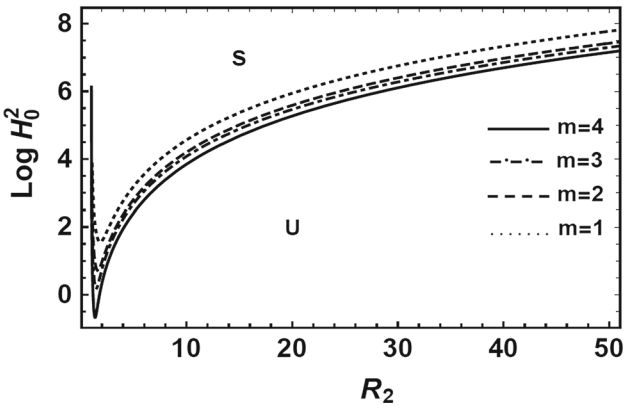

Figure 3. Plots of the linear stability given in eq. (49) for different values of m.

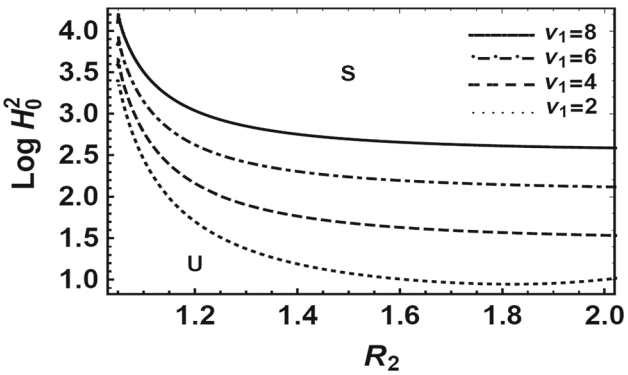

Figure 4. Plots of the linear stability given in eq. (49), for different values of ν_1.

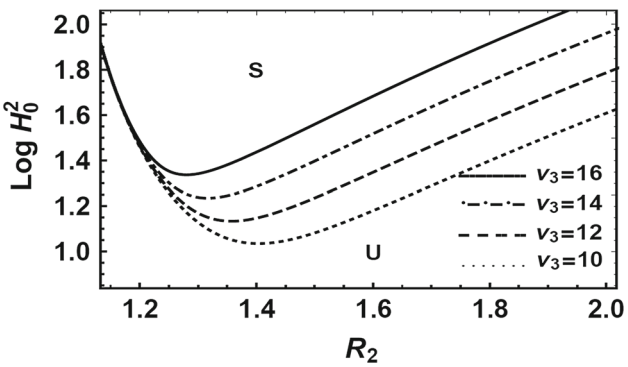

Figure 5. Plots of the linear stability given in eq. (49) for different values of ν_3.

influence of any parameter, it is only enough to use the curve that divides the stability and instability regions. Accordingly, figure 3 is plotted to display the impact of the azimuthal parameter m on the stability configuration. All other parameters are chosen as in figure 2 except m which varies. As shown in this figure, the increase in the parameter m increases the stable region. This result corresponds to that confirmed earlier in the previous work of El-Dib [37]. Additionally, the result is in good agreement with the result obtained earlier, for the axial disturbance, by Chandrasekhar [34]. On the other hand, as the outer radius is increased, the system tends to be more destabilising. As seen, the stabilising influence occurs at small values of R_2. Once more, this mechanism seems to be in relevance to the comprehensive work that was earlier given by Rüdiger *et al* [38].

Figures 4 and 5 are depicted to indicate the influences of the ratio of Darcy's coefficients ν_1 and ν_3. It is observed that ν_1 and ν_3 have destabilising effects. This result is in good agreement with the result that has been recently confirmed by Moatimid *et al* [10]. Figure 6 is plotted to display the impact of the ratio of the frequency parameter Ω_3 on the stability picture. In this figure, all the physical parameters are fixed, except Ω_3. It is observed that the stable region decreases as Ω_3 increases. Therefore, one may say that Ω_3 has destabilising effects. Similar results have been obtained earlier by El-Dib and Moatimid [36]. Finally, figure 7 is depicted to indicate the influence of the ratio of the densities ρ_1. It is observed that ρ_1 has destabilising effects. The influence is increased for small values of R_2.

To study the effect of nonlinear stability on the amplitude modulation of the progressive waves, eqs (38a) and (38b) are to be considerd. The treatment of these equations may be achieved through the following perturbation technique.

4. The nonlinear stability approach

The nonlinear stability procedure given by eqs (38a) and (38b) had been discussed in detail in the theoretical work by El-Dib [26]. The current work will discuss the coupled nonlinear dispersion equations in a general form. Therefore, separating the real and imaginary parts is needed. Following a similar procedure as given before,

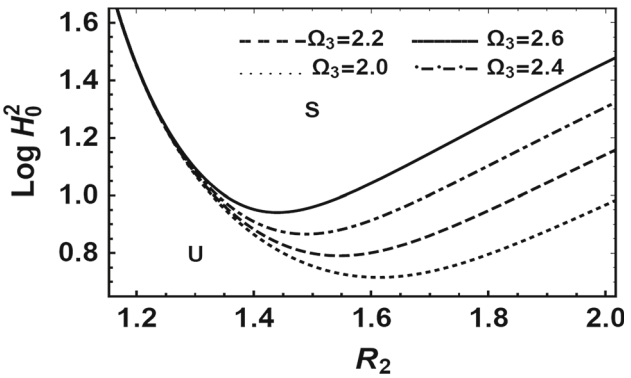

Figure 6. Plots of the linear stability given in eq. (49), for different values of Ω_3.

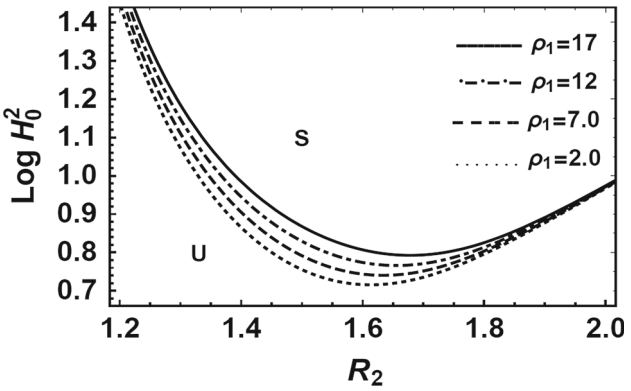

Figure 7. Plots of the linear stability given in eq. (49), for different values of ρ_1.

the calculations are lengthy, but straightforward. This procedure gives the following nonlinear characteristic differential equation:

$$\tilde{L}_1\eta + \tilde{L}_2\xi = \tilde{N}_1(\eta,\xi) \tag{51a}$$

and

$$\tilde{L}_3\eta + \tilde{L}_4\xi = \tilde{N}_2(\eta,\xi), \tag{51b}$$

where the operator $\tilde{L}_i$ is defined as

$$\tilde{L} = \tilde{a}_i\frac{\partial^2}{\partial t^2} + \tilde{b}_i\frac{\partial^2}{\partial\theta^2} + \tilde{c}_i\frac{\partial^2}{\partial\theta\partial t} + \tilde{g}_i\frac{\partial}{\partial\theta}.$$

In addition, the nonlinear terms, $\tilde{N}_1(\eta,\xi)$ and $\tilde{N}_2(\eta,\xi)$, represent all the quadratic and cubic terms in the variables η and ξ and $\tilde{a}_i$, $\tilde{b}_i$, $\tilde{c}_i$ and $\tilde{g}_i$ are constant coefficients, which are well-known from the background of the paper. To avoid the length of the paper, they will be omitted.

For this purpose, eqs (51a) and (51b) may be rewritten in the following form:

$$L\eta = \tilde{L}_4\tilde{N}_1 - \tilde{L}_2\tilde{N}_2 \tag{52a}$$

and

$$L\xi = \tilde{L}_1\tilde{N}_2 - \tilde{L}_3\tilde{N}_1, \tag{52b}$$

where

$$L = \tilde{L}_1\tilde{L}_4 - \tilde{L}_2\tilde{L}_3.$$

The following analysis will be based on the multiple time-scale technique given in the previous work of El-Dib [26]. This technique depends mainly on the small parameter δ. It measures the ratio of a typical wavelength, or periodic time relative to a typical length, or the time-scale of modulation. Therefore, one assumes that δ is a small parameter that characterises the slow modulation. In view of this approach, the independent variables θ and t, which are measured on the scale of the typical wavelength and period time, can be extended to introduce alternative, independent variables,

$$\Theta_n = \delta^n\theta \quad \text{and} \quad T_n = \delta^n t, \quad n = 0, 1, 2, ... \tag{53}$$

The uniform monochromatic wave train solutions to (52a) and (52b) are in the following form:

$$\eta(\theta,t) = \gamma_1^{i(m\theta-\omega t)} + \text{c.c.} \tag{54a}$$

and

$$\xi(\theta,t) = \gamma_2 e^{i(m\theta-\omega t)} + \text{c.c.} \tag{54b}$$

Let Θ_0, T_0 be the appropriate variety of fast variations and Θ_1, T_1, Θ_2 and T_2 are the slow ones. The differential operators can now be expressed as the derivative expansions

$$\frac{\partial}{\partial\theta} = m\frac{\partial}{\partial\kappa} + \delta\frac{\partial}{\partial\Theta_1} + \delta^2\frac{\partial}{\partial\Theta_2} + \cdots$$

and

$$\frac{\partial}{\partial t} = -\omega\frac{\partial}{\partial\kappa} + \delta\frac{\partial}{\partial T_1} + \delta^2\frac{\partial}{\partial T_2} + \cdots, \tag{55}$$

where $\kappa = m\Theta_0 - \omega T_0$ refers to the lowest order.

It is more convenient to expand the operator $\tilde{L}$ in the following form:

$$L\left(im, -i\omega + i\delta\left(\frac{\partial}{\partial\Theta_1}, \frac{\partial}{\partial T_1}\right) + i\delta^2\left(\frac{\partial}{\partial\Theta_2}, \frac{\partial}{\partial T_2}\right) + \cdots\right). \tag{56}$$

The expression of the operator L can be expanded in powers of δ. Using Taylor's theorem about $(m, -\omega)$, one retains only the terms up to $O(\delta^2)$. Therefore, one gets

$$L \to \hat{L}_0 + \delta\hat{L}_1 + \delta^2\hat{L}_2 + \cdots \tag{57}$$

where

$$\hat{L}_0 \equiv (m-\omega)\frac{\partial}{\partial\kappa}, \tag{58a}$$

$$\hat{L}_1 \equiv i\left(\frac{\partial \hat{L}_0}{\partial \omega}\right)\frac{\partial}{\partial T_1} - i\left(\frac{\partial \hat{L}_0}{\partial m}\right)\frac{\partial}{\partial \Theta_1} \tag{58b}$$

and

$$\hat{L}_2 \equiv i\left(\frac{\partial \hat{L}_0}{\partial \omega}\right)\frac{\partial}{\partial T_2} - i\left(\frac{\partial \hat{L}_0}{\partial m}\right)\frac{\partial}{\partial \Theta_2} - \frac{1}{2}\left(\frac{\partial^2 \hat{L}_0}{\partial \omega^2}\right)\frac{\partial^2}{\partial T_1^2} - \frac{1}{2}\left(\frac{\partial^2 \hat{L}_0}{\partial m^2}\right)\frac{\partial^2}{\partial \Theta_1^2} + \frac{1}{2}\left(\frac{\partial^2 \hat{L}_0}{\partial m \partial \omega}\right)\frac{\partial^2}{\partial \Theta_1 \partial T_1}. \tag{58c}$$

Expressing the expansion of operator (57) into eqs (54a) and (54b), one finds

$$\left(\hat{L}_0 + \delta \hat{L}_1 + \delta^2 \hat{L}_2\right)(\eta, \xi) = 0, \tag{59}$$

The foregoing analysis follows a perturbation procedure to obtain a uniform valid solution. Actually, this treatment requires the cancellation of the secular terms. As stated before, this procedure was introduced in detail by El-Dib [26]. It is well known that the coupled nonlinear Schrödinger equations are described in the light of the unidirectional wave modulation. They have been used to describe the spatial and temporal evolution of the envelope of a sinusoidal wave with phase $(m\theta - \omega t)$. Therefore, following similar arguments as that given by El-Dib [26], one finds the following coupled nonlinear Schrödinger equations

$$i\frac{\partial \gamma_1}{\partial \tau} + P\frac{\partial^2 \gamma_1}{\partial \zeta^2} = \sum_{j=1}^{2}\left(Q_{1j}\gamma_j^2\overline{\gamma}_j + Q_{1j+1}\gamma_j^2\overline{\gamma}_{3-j} + Q_{1j+3}\gamma_1\gamma_2\overline{\gamma}_j\right) \tag{60a}$$

and

$$i\frac{\partial \gamma_2}{\partial \tau} + P\frac{\partial^2 \gamma_2}{\partial \zeta^2} = \sum_{j=1}^{2}\left(Q_{2j}\gamma_j^2\overline{\gamma}_j + Q_{2j+1}\gamma_j^2\overline{\gamma}_{3-j} + Q_{2j+3}\gamma_1\gamma_2\overline{\gamma}_j\right), \tag{60b}$$

where $\overline{\gamma}_j$ is the complex conjugate of γ_j,

$$P = \frac{1}{2}\frac{\mathrm{d}V_g}{\mathrm{d}m}, \quad \zeta = \delta(\theta - V_g t)$$

and

$$\tau = \delta^2 t.$$

The group velocity may be written as

$$V_g = -\frac{\partial D}{\partial m}\left(\frac{\partial D}{\partial \omega}\right)^{-1}$$

and $Q_{i(j+n)}$ are constant coefficients. They will be known from the background of the paper. To avoid the length of the paper, they will be omitted.

The stability criterion of the coupled nonlinear Schrödinger equations (60a) and (60b) has been derived by El-Dib [26]. He showed that the perturbation is stable in accordance with the following condition:

$$PS > 0, \tag{61}$$

where

$$S = L_2^2\left(Q_{11} + Q_{23} + Q_{25}\right) + L_1^2\left(Q_{14} + Q_{16} + Q_{22}\right).$$

Condition (61) can be rewritten as follows:

$$\frac{E_9(H_0^2)^9 + E_8(H_0^2)^8 + E_7(H_0^2)^7 + E_6(H_0^2)^6 + E_5(H_0^2)^5}{F_2(H_0^2)^2 + F_1H_0^2 + F_0} + \frac{+E_4(H_0^2)^4 + E_3(H_0^2)^3 + E_2(H_0^2)^2 + E_1H_0^2 + E_0}{F_2(H_0^2)^2 + F_1H_0^2 + F_0} > 0, \tag{62}$$

where E_i and F_j are constant coefficients, which are well-known from the background of the paper. To avoid the length of the paper, they will be omitted.

The stability criterion requires that the quotient in the right-hand side of inequality (61) is a positive value. This may happen if the product of the numerator and denominator becomes positive. Subsequently, in light of the nonlinear theory approach, the system is stable provided that the following condition holds:

$$\left(E_9(H_0^2)^9 + E_8(H_0^2)^8 + E_7(H_0^2)^7 + E_6(H_0^2)^6 + E_5(H_0^2)^5 + E_4(H_0^2)^4 + E_3(H_0^2)^3 + E_2(H_0^2)^2 + E_1H_0^2 + E_0\right)\left(F_2(H_0^2)^2 + F_1H_0^2 + F_0\right) > 0, \tag{63a}$$

which is a polynomial of the eleventh degree in H_0^2.

In addition, the following criterion is necessary:

$$F_2H_0^4 + F_1H_0^2 + F_0 = 0. \tag{63b}$$

Condition (63b) is sometimes called the resonance curves. Otherwise, the system becomes unstable.

Now, for more convenience, a numerical calculation of the stability criteria given by relations (63a) and (63b) will be made. Consider a similar treatment presented in §3 to evaluate the above stability criteria in a non-dimensional form. Therefore, one may assume the previous characteristics that were given in §3.

In order to illustrate the stability criteria throughout the nonlinear stability approach, some graphs must be plotted. Typically, it is convenient to plot $\log H_0^2$ vs. the radius R_2. As previously shown, the stable region is denoted by the letter S. Simultaneously, letter U stands for the unstable one. The numerical calculations showed that the eleventh roots of H_0^2 (see table 1).

Therefore, in view of the nonlinear stability criteria, figure 8 plots only three transition curves. The stability/instability is checked from inequality (63a). As shown in this figure, the plane is divided into several

Table 1. The eleventh roots of H_0^2.

Equation	Number of roots	Nature of the roots	Result
63a	One	Real and negative	It has no implication
	Four	Complex conjugates	They have no implication
	Six	Positive values; three of the curves are integrated with the other three, and result in only three curves	Three transition curves are only presented in the graph
63b	Two	Complex conjugates	They have no implication

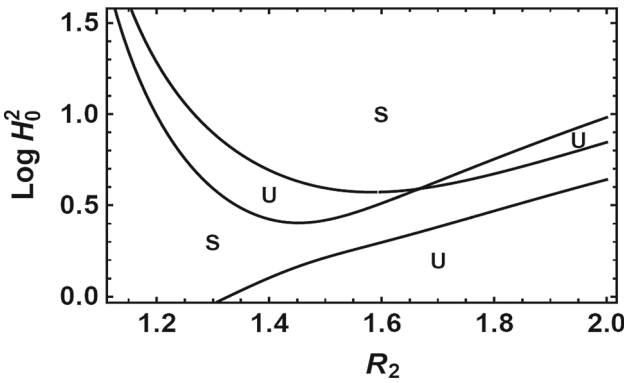

Figure 8. Plots of the nonlinear stability given in (63a) and (63b).

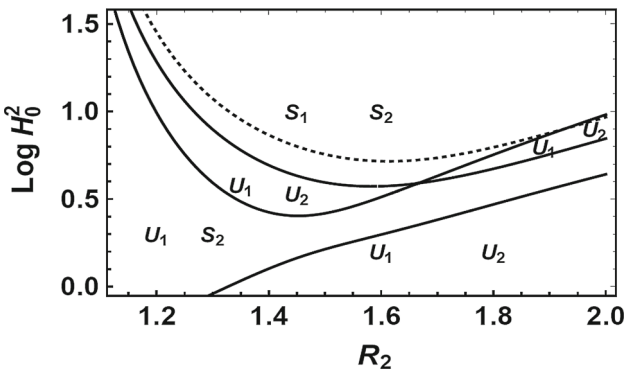

Figure 9. Plots of the linear and nonlinear stability given in (49), (63a) and (63b).

parts of stability/instability. These curves partitioned the plane into stable and unstable parts. This means that the nonlinear stability becomes more accurate in the stability theory. In each region, the coordinates of any point that satisfies inequality (63b) is stable. Otherwise, it becomes an unstable region.

It is more convenient to merge the linear and nonlinear stability criteria in one figure. Therefore, the stable and unstable regions in the linear case are denoted by the letters S_1 and U_1, respectively. On the other hand, throughout the nonlinear approach, these regions are labelled by letters S_2 and U_2. In the linear case, the curve of equality of (49) is pictured as a dotted curve. Meanwhile, nonlinear condition (63a) is plotted to give three solid curves. Figure 9 is depicted to show the linear/nonlinear transition curves. As seen from this figure, the linear curve is still controlling the stability of the system. Consequently, the previous concepts that are illustrated throughout the linear theory approach are still valid even in the nonlinear approach.

5. Concluding remarks

The current paper investigates the linear, as well as nonlinear stability analysis of two rotating cylindrical interfaces, separated by three perfect, homogeneous and incompressible magnetic fluids. The system is influenced by a uniform azimuthal magnetic field. In accordance with the importance of the porous media, the work examines a few representative porous media. The nonlinear approach is accomplished from the linear solutions of the governing equations of motion together with the appropriate nonlinear boundary conditions. To relax the mathematical manipulation, a simplified formulation is considered to yield coupled characteristic nonlinear partial differential equations of the deflections of the surface waves with complex coefficients. As a special case, by ignoring the nonlinear terms, the linear stability criteria have been obtained. Because the surface deflections are real, the separation of variables is utilised. This procedure helped us to get rid of the damping terms. It follows that the stability criteria are conducted. It also follows that the linear dispersion relation gives quadratic equation in the square of the frequency of the surface wave. Following El-Dib [26], the nonlinear characteristic equations are analysed along with the nonlinear Schrödinger equation. These equations are controlled by the nonlinear stability criterion of the system. These conditions are illustrated graphically using a set of figures. The influences of some physical parameters are also shown. The concluding remarks may be drawn along the following points:

1. The investigation of the linear stability analysis yields the following:
   (a) Away from the case of a single interface, the current situation resulted in a quadratic equation of the square of the growth rate of the surface waves.

(b) The linear dispersion relation is given by eq. (44). This equation resulted in several transition curves.
(c) As given by El-Dib [37], it is found that the increase in the azimuthal wave number plays a stabilising influence on the stability configuration. Simultaneously, the unstable mechanism of the outer radius seems to be in relevance to the comprehensive work given by Rüdiger *et al* [38].
(d) The influence of the ratio of Darcy's coefficients ν_1 and ν_3 plays a destabilising effect. This result is in agreement with the previous results achieved by Moatimid *et al* [10].
(e) The effect of the ratio of the frequency parameter Ω_3 plays a destabilising influence on the stability configuration. Similar results have been obtained earlier by El-Dib and Moatimid [36].
(f) The ratio of the densities ρ_1 has a destabilising effect.

2. The analysis of the nonlinear stability analysis yields the following:
(a) The analysis yields coupled nonlinear characteristic equations appearing in eqs (38a) and (38b).
(b) Following El-Dib [26], one finds the coupled nonlinear Schrödinger equation as given in eqs (60a) and (60b).
(c) The transition curves yield a polynomial of the eleventh degree in H_0^2 together with resonance quadratic polynomial in H_0^2.
(d) The numerical calculations in light of a chosen sample system, divided the stability picture into several parts of stability/instability. This shows the accuracy of the nonlinear approach.
(e) On merging the linear/nonlinear curves, one finds that the linear curve is still controlling the stability configuration.

Appendix

The coefficients appearing in eqs (27) and (28) may be listed as follows:

$$L_1 \equiv a_1\frac{\partial^2}{\partial t^2}+b_1\frac{\partial^2}{\partial\theta^2}+c_1\frac{\partial^2}{\partial\theta\,\partial t}+(h_1+ik_1)\frac{\partial}{\partial t}+(g_1+if_1)\frac{\partial}{\partial\theta}$$

$$\begin{aligned}
a_1 &= 2m^2R_1^{13}R_2^4\left((\mu_1-\mu_2)^2(\mu_2-\mu_3)^2R_1^{4m}\right.\\
&\quad +2(\mu_1^2-\mu_2^2)(\mu_2^2-\mu_3^2)R_1^{2m}R_2^{2m}\\
&\quad \left.+(\mu_1+\mu_2)^2(\mu_2+\mu_3)^2R_2^{4m}\right)\\
&\quad \times\left((\rho_1-\rho_2)R_1^{4m}\right.\\
&\quad \left.-2\rho_1R_1^{2m}R_2^{2m}+(\rho_1+\rho_2)R_2^{4m}\right),\\
b_1 &= -2T_1m^2R_1^{10}R_2^4(R_1^{2m}-R_2^{2m})\left((\mu_1-\mu_2)^2(\mu_2\right.\\
&\quad \left.-\mu_3)^2R_1^{4m}+2(\mu_1^2-\mu_2^2)(\mu_2^2-\mu_3^2)R_1^{2m}R_2^{2m}\right.\\
&\quad \left.+(\mu_1+\mu_2)^2(\mu_2+\mu_3)^2R_2^{4m}\right),\\
c_1 &= 2m^2R_1^{13}R_2^4\left((\mu_1-\mu_2)^2(\mu_2-\mu_3)^2R_1^{4m}\right.\\
&\quad +2(\mu_1^2-\mu_2^2)(\mu_2^2-\mu_3^2)R_1^{2m}R_2^{2m}\\
&\quad \left.+(\mu_1+\mu_2)^2(\mu_2+\mu_3)^2R_2^{4m}\right)\\
&\quad \times\left((\rho_1\Omega_1-\rho_2\Omega_2)R_1^{4m}-2\rho_1\Omega_1R_1^{2m}R_2^{2m}\right.\\
&\quad \left.+(\rho_1\Omega_1+\rho_2\Omega_2)R_2^{4m}\right),\\
h_1 &= 2m^2R_1^{13}R_2^4(R_1^{2m}-R_2^{2m})\\
&\quad \times\left((\mu_1-\mu_2)(\mu_2-\mu_3)R_1^{2m}\right.\\
&\quad \left.+(\mu_1+\mu_2)(\mu_2+\mu_3)R_2^{2m}\right)^2\\
&\quad \times\left((\rho_1\nu_1-\rho_2\nu_2)R_1^{2m}-(\rho_1\nu_1)\right.\\
&\quad \left.+\rho_2\nu_2)R_2^{2m}\right.\\
k_1 &= 2m^2R_1^{13}R_2^4(R_1^{2m}-R_2^{2m})\left((\mu_1-\mu_2)\right.\\
&\quad \left.\times(\mu_2-\mu_3)R_1^{2m}+(\mu_1+\mu_2)(\mu_2+\mu_3)R_2^{2m}\right)^2\\
&\quad \times\left((m-2)(\rho_1\Omega_1-\rho_2\Omega_2)R_1^{2m}\right.\\
&\quad \left.-((m-2)\rho_1\Omega_1+(m+2)\rho_2\Omega_2)R_2^{2m}\right),\\
g_1 &= 2m^2R_1^{13}R_2^4(R_1^{2m}-R_2^{2m})\left((\mu_1-\mu_2)\right.\\
&\quad \left.\times(\mu_2-\mu_3)R_1^{2m}+(\mu_1+\mu_2)(\mu_2+\mu_3)R_2^{2m}\right)^2\\
&\quad \times\left((\rho_1\nu_1\Omega_1-\rho_2\nu_2\Omega_2)R_1^{2m}\right.\\
&\quad \left.-(\rho_1\nu_1\Omega_1+\rho_2\nu_2\Omega_2)R_2^{2m}\right)\\
f_1 &= -2m^2R_1^{11}R_2^4(R_1^{2m}-R_2^{2m})\left((\mu_1-\mu_2)\right.\\
&\quad \left.\times(\mu_2-\mu_3)R_1^{2m}+(\mu_1+\mu_2)(\mu_2+\mu_3)R_2^{2m}\right)\\
&\quad \times\left(mH_0^2(R_1^{2m}-R_2^{2m})(\mu_1-\mu_2)^2\right.\\
&\quad \times\left((\mu_2-\mu_3)R_1^{2m}+(\mu_2+\mu_3)R_2^{2m}\right)\\
&\quad -R_1^2\left((\mu_1-\mu_2)(\mu_2-\mu_3)R_1^{2m}\right.\\
&\quad \left.+(\mu_1+\mu_2)(\mu_2+\mu_3)R_2^{2m}\right)\left((m-2)(\rho_1\Omega_1^2\right.\\
&\quad -\rho_2\Omega_2^2)R_1^{2m}-((m-2)\rho_1\Omega_1^2\\
&\quad \left.\left.+(m+2)\rho_2\Omega_2^2)R_2^{2m}\right)\right),
\end{aligned}$$

$$
\begin{aligned}
L_2 \equiv\ & a_2\frac{\partial^2}{\partial t^2}+b_2\frac{\partial^2}{\partial\theta^2}\\
&+c_2\frac{\partial^2}{\partial\theta\,\partial t}+(h_2+ik_2)\frac{\partial}{\partial t}+(g_2+if_2)\frac{\partial}{\partial\theta}\\
a_2 =\ & 2m^2R_1^{12+m}R_2^{5+m}\left((\mu_1-\mu_2)^2(\mu_2-\mu_3)^2R_1^{4m}\right.\\
&+2(\mu_1^2-\mu_2^2)(\mu_2^2-\mu_3^2)R_1^{2m}R_2^{2m}\\
&\left.+(\mu_1+\mu_2)^2(\mu_2+\mu_3)^2R_2^{4m}\right)\rho_2,\\
b_2 =\ & 0,\\
c_2 =\ & 4m^2R_1^{12+m}R_2^{5+m}(R_1^{2m}-R_2^{2m})\left((\mu_1-\mu_2)^2(\mu_2\right.\\
&-\mu_3)^2R_1^{4m}+2(\mu_1^2-\mu_2^2)(\mu_2^2-\mu_3^2)R_1^{2m}R_2^{2m}\\
&\left.+(\mu_1+\mu_2)^2(\mu_2+\mu_3)^2R_2^{4m}\right)\rho_2\Omega_2,\\
h_2 =\ & \nu_2c_2/\Omega_2\\
k_2 =\ & mc_2\\
g_2 =\ & 4m^2R_1^{12+m}R_2^{5+m}(R_1^{2m}-R_2^{2m})\\
&\times\left((\mu_1-\mu_2)(\mu_2-\mu_3)R_1^{2m}\right.\\
&\left.+(\mu_1+\mu_2)(\mu_2+\mu_3)R_2^{2m}\right)^2\rho_2\nu_2\Omega_2,\\
f_2 =\ & -4m^3R_1^{11+m}R_2^{4+m}(R_1^{2m}-R_2^{2m})\\
&\times\left((\mu_1-\mu_2)(\mu_2-\mu_3)R_1^{2m}\right.\\
&\left.+(\mu_1+\mu_2)(\mu_2+\mu_3)R_2^{2m}\right)\\
&\times\left(H_0^2(R_1^{2m}-R_2^{2m})(\mu_1-\mu_2)(\mu_2-\mu_3)\right.\\
&-R_1R_2\left((\mu_1-\mu_2)(\mu_2-\mu_3)R_1^{2m}\right.\\
&\left.\left.+(\mu_1+\mu_2)(\mu_2+\mu_3)R_2^{2m}\right)\rho_2\Omega_2^2\right),\\
L_3 \equiv\ & a_3\frac{\partial^2}{\partial t^2}+b_3\frac{\partial^2}{\partial\theta^2}\\
&+c_3\frac{\partial^2}{\partial\theta\,\partial t}+(h_3+ik_3)\frac{\partial}{\partial t}+(g_3+if_3)\frac{\partial}{\partial\theta}\\
a_3 =\ & 4m^2R_1^{5+m}R_2^{12+m}(R_1^{2m}-R_2^{2m})\left((\mu_1-\mu_2)^2(\mu_2\right.\\
&-\mu_3)^2R_1^{4m}+2(\mu_1^2-\mu_2^2)(\mu_2^2-\mu_3^2)R_1^{2m}R_2^{2m}\\
&\left.+(\mu_1+\mu_2)^2(\mu_2+\mu_3)^2R_2^{4m}\right)\rho_2,\\
b_3 =\ & 0,\\
c_3 =\ & 4m^2R_1^{5+m}R_2^{12+m}(R_1^{2m}-R_2^{2m})\left((\mu_1-\mu_2)^2(\mu_2\right.\\
&-\mu_3)^2R_1^{4m}+2(\mu_1^2-\mu_2^2)(\mu_2^2-\mu_3^2)R_1^{2m}R_2^{2m}\\
&\left.+(\mu_1+\mu_2)^2(\mu_2+\mu_3)^2R_2^{4m}\right)\rho_2\Omega_2,\\
h_3 =\ & 4m^2R_1^{5+m}R_2^{12+m}(R_1^{2m}-R_2^{2m})\\
&\times\left((\mu_1-\mu_2)(\mu_2-\mu_3)R_1^{2m}\right.\\
&\left.+(\mu_1+\mu_2)(\mu_2+\mu_3)R_2^{2m}\right)^2\rho_2\nu_2,\\
k_3 =\ & m\Omega_2h_3/\nu_2,\\
g_3 =\ & h_3\Omega_2,\\
f_3 =\ & -4m^3R_1^{4+m}R_2^{11+m}(R_1^{2m}-R_2^{2m})\left((\mu_1-\mu_2)(\mu_2\right.\\
&-\mu_3)R_1^{2m}+(\mu_1+\mu_2)(\mu_2+\mu_3)R_2^{2m}\left.\right)\left(H_0^2(R_1^{2m}\right.\\
&-R_2^{2m})\mu_2(\mu_1-\mu_2)(\mu_2-\mu_3)\\
&-R_1R_2\left((\mu_1-\mu_2)(\mu_2-\mu_3)R_1^{2m}\right.\\
&\left.\left.+(\mu_1+\mu_2)(\mu_2+\mu_3)R_2^{2m}\right)\rho_2\Omega_2^2\right),\\
L_4 \equiv\ & a_4\frac{\partial^2}{\partial t^2}+b_4\frac{\partial^2}{\partial\theta^2}+c_4\frac{\partial^2}{\partial\theta\,\partial t}\\
&+(h_4+ik_4)\frac{\partial}{\partial t}+(g_4+if_4)\frac{\partial}{\partial\theta}\\
a_4 =\ & 2m^2R_1^4R_2^{13}\left((\mu_1-\mu_2)^2(\mu_2-\mu_3)^2R_1^{4m}\right.\\
&+2(\mu_1^2-\mu_2^2)(\mu_2^2-\mu_3^2)R_1^{2m}R_2^{2m}\\
&\left.+(\mu_1+\mu_2)^2(\mu_2+\mu_3)^2R_2^{4m}\right)\\
&\times\left((\rho_3-\rho_2)R_1^{4m}-2\rho_3R_1^{2m}R_2^{2m}\right.\\
&\left.+(\rho_1+\rho_3)R_2^{4m}\right),\\
b_4 =\ & -2T_2m^2R_1^4R_2^{10}(R_1^{2m}-R_2^{2m})\left((\mu_1-\mu_2)^2(\mu_2\right.\\
&-\mu_3)^2R_1^{4m}+2(\mu_1^2-\mu_2^2)(\mu_2^2-\mu_3^2)R_1^{2m}R_2^{2m}\\
&\left.+(\mu_1+\mu_2)^2(\mu_2+\mu_3)^2R_2^{4m}\right),\\
c_4 =\ & 2m^2R_1^4R_2^{13}\left((\mu_1-\mu_2)^2(\mu_2-\mu_3)^2R_1^{4m}\right.\\
&+2(\mu_1^2-\mu_2^2)(\mu_2^2-\mu_3^2)R_1^{2m}R_2^{2m}\\
&\left.+(\mu_1+\mu_2)^2(\mu_2+\mu_3)^2R_2^{4m}\right)\\
&\times\left((\rho_3\Omega_3-\rho_2\Omega_2)R_1^{4m}-2\rho_3\Omega_3R_1^{2m}R_2^{2m}\right.\\
&\left.+(\rho_3\Omega_3+\rho_2\Omega_2)R_2^{4m}\right),\\
h_4 =\ & 2m^2R_1^4R_2^{13}(R_1^{2m}-R_2^{2m})\\
&\times\left((\mu_1-\mu_2)(\mu_2-\mu_3)R_1^{2m}+(\mu_1\right.\\
&\left.+\mu_2)(\mu_2+\mu_3)R_2^{2m}\right)^2\left((\rho_2\nu_2\right.\\
&\left.-\rho_3\nu_3)R_1^{2m}+(\rho_2\nu_2+\rho_3\nu_3)R_2^{2m}\right),\\
k_4 =\ & 2m^2R_1^4R_2^{13}(R_1^{2m}-R_2^{2m})\left((\mu_1-\mu_2)(\mu_2\right.\\
&\left.-\mu_3)R_1^{2m}+(\mu_1+\mu_2)(\mu_2+\mu_3)R_2^{2m}\right)^2\\
&\times\left((m+2)(\rho_2\Omega_2-\rho_3\Omega_3)R_1^{2m}\right.\\
&\left.+((m-2)\rho_2\Omega_2+(m+2)\rho_3\Omega_3)R_2^{2m}\right),\\
g_4 =\ & -2m^2R_1^4R_2^{11}(R_1^{2m}-R_2^{2m})\\
&\times\left((\mu_1-\mu_2)(\mu_2-\mu_3)R_1^{2m}\right.\\
&\left.+(\mu_1+\mu_2)(\mu_2+\mu_3)R_2^{2m}\right)^2\\
&\times\left((\rho_2\nu_2\Omega_2-\rho_3\nu_3\Omega_3)R_1^{2m}\right.\\
&\left.+(\rho_2\nu_2\Omega_2+\rho_3\nu_3\Omega_3)R_2^{2m}\right),
\end{aligned}
$$

and

$$
\begin{aligned}
f_4 =\ & -2m^2R_1^4R_2^{11}(R_1^{2m}-R_2^{2m})\\
&\times\left((\mu_1-\mu_2)(\mu_2-\mu_3)R_1^{2m}\right.\\
&\left.+(\mu_1+\mu_2)(\mu_2+\mu_3)R_2^{2m}\right)\\
&\times\left(mH_0^2(R_1^{2m}-R_2^{2m})(\mu_2\right.
\end{aligned}
$$

$$
\begin{aligned}
&-\mu_3)^2\left((\mu_1-\mu_2)R_1^{2m}(\mu_1+\mu_2)R_2^{2m}\right)\\
&-R_2^2\left((\mu_1-\mu_2)(\mu_2-\mu_3)R_1^{2m}\right.\\
&\left.+(\mu_1+\mu_2)(\mu_2+\mu_3)R_2^{2m}\right)\\
&\times\left((m+2)(\rho_2\Omega_2^2-\rho_3\Omega_3^2)R_1^{2m}\right.\\
&\left.+((m-2)\rho_2\Omega_2^2+(m+2)\rho_3\Omega_3^2)R_2^{2m}\right).
\end{aligned}
$$

References

[1] J M D Coey, *Magnetism and magnetic material* (Cambridge University Press, New York, 2009)
[2] R E Rosensweig, *Adv. Electron. Electron. Phys.* **48**, 103 (1979)
[3] R E Zelazo and J R Melcher, *J. Fluid Mech.* **39**, 1 (1969)
[4] S K Malik and M Singh, *Quart. Appl. Math.* **47**, 59 (1989)
[5] A R F Elhefnawy, M A A Mahmoud and G M Khedr, *Can. Appl. Math. Q* **12**, 323 (2004)
[6] Y O El-Dib, G M Moatimid and A A Mady, *Pramana – J. Phys.* **93**: 82 (2019)
[7] H H Bau, *Phys. Fluids* **25**, 1719 (1982)
[8] K Zakaria, M A Sirwah and S A Alkharashi, *Phys. Scr.* **77**, 025401 (2008)
[9] S A Al-Karashi and Y Gamiel, *Theor. Math. Phys.* **191**, 580 (2017)
[10] G M Moatimid, Y O El-Dib and M H Zekry, *Chin. J. Phys.* **56**, 2507 (2018)
[11] G M Moatimid, Y O El-Dib and M H Zekry, *Pramana – J. Phys.* **92**: 22 (2019)
[12] G M Moatimid, N T Eldabe and A Sayed, *Heat Transfer - Asian Res.* **48**, 4074 (2019)
[13] N E Kochin, I A Kibel and N V Roze, *Theoretical hydromechanics* (Interscience, New York, 1965)
[14] G I Taylor, *Phil. Trans. R. Soc. A* **223**, 289 (1923)
[15] J L Synge, *Proc. R. Soc. A* **167**, 250 (1938)
[16] M V Abakumov, *Comput. Math. Math. Phys.* **59**, 584 (2019)
[17] V Ya Rudyak and E G Bord, *Fluid Dyn.* **53**, 729 (2018)
[18] Y O El-Dib and A A Mady, *J. Comput. Appl. Mech.* **49**, 261 (2018)
[19] D Lu, A R Seadawy, J Wang, M Arshad and U Farooq, *Pramana – J. Phys*. **93**: 44 (2019)
[20] W Liu and Y Zhang, *Opt. Quant. Electron*. **51**, 65 (2019)
[21] M Asadzadeh and C Standard, *J. Math. Sci.* **239**, 233 (2019)
[22] A H Nayfeh, *J. Appl. Mech.* **43**, 584 (1976)
[23] A R F Elhefnawy, *ZAMM* **77**, 19 (1997)
[24] D S Lee, *Eur. Phy. J. B* **28**, 495 (2002)
[25] K Zakaria, *Physica A* **327**, 221 (2003)
[26] Y O El-Dib, *Nonlinear Dyn.* **24**, 399 (2001)
[27] G M Moatimid, *J. Phys. A* **36**, 11343 (2003)
[28] A RF Elhefnawy, G M Moatimid and A K Elcoot, *ZAMP* **55**, 63 (2004)
[29] M Eghbali and B Farokhi, *Pramana – J. Phys.* **84**, 637 (2015)
[30] A R Seadawy and K El-Rashidy, *Pramana – J. Phys.* **87**: 20 (2016)
[31] J Zhang, W Hu and Y Ma, *Pramana – J. Phys.* **87**: 93 (2016)
[32] G M Moatimid, Y O El-Dib and M H Zekry, *Arabian J. Sci. Eng.* **45**, 391 (2020)
[33] Y O El-Dib, G M Moatimid and A A Mady, *Chin. J. Phys.* **66**, 285 (2020)
[34] S Chandrasekhar, *Hydrodynamic and hydromagnetic stability* (Clarendon Press, Oxford, 1961)
[35] J R Melcher, *Field coupled surface waves* (MIT Press, Cambridge, 1963)
[36] Y O El-Dib and G M Moatimid, *Z. Naturforsch. A* **57a**, 159 (2002)
[37] Y O El-Dib, *J. Phys. A* **30**, 3585 (1997)
[38] G Rüdiger, M Geller, R Hollerbach, M Schultz and F Stefani, *Phys. Rep*. **741**, 1 (2018)